

UNIVERSIDAD DE LOS ANDES

THESIS

---

# Two-Photon Imaging Using Tunable Spatial Correlations

---

*Author:*  
Juan VARGAS

*Supervisor:*  
Dr. Alejandra VALENCIA

*A thesis submitted in fulfillment of the requirements  
for the degree of Physicist*

*in the*

Quantum Optics  
Physics Department



April 17, 2018

## Declaration of Authorship

I, Juan VARGAS, declare that this thesis titled, "Two-Photon Imaging Using Tunable Spatial Correlations" and the work presented in it are my own. I confirm that:

- This work was done wholly or mainly while in candidature for a research degree at this University.
- Where any part of this thesis has previously been submitted for a degree or any other qualification at this University or any other institution, this has been clearly stated.
- Where I have consulted the published work of others, this is always clearly attributed.
- Where I have quoted from the work of others, the source is always given. With the exception of such quotations, this thesis is entirely my own work.
- I have acknowledged all main sources of help.
- Where the thesis is based on work done by myself jointly with others, I have made clear exactly what was done by others and what I have contributed myself.

Signed:

---

Date:

---

*"Nonesenses... later due"*

N.N

UNIVERSIDAD DE LOS ANDES

*Abstract*

Science Faculty  
Physics Department

Physicist

**Two-Photon Imaging Using Tunable Spatial Correlations**

by Juan VARGAS

Two-Photon Imaging is a well studied phenomena, where we take advantage of the different correlations in which the light can be related to reconstruct the image of certain objects. In this Thesis use different spatial correlations of a SPDC light source, where we change this correlations changing the pump waist.

## *Acknowledgements*

The acknowledgments and the people to thank go here, don't forget to include your project advisor... s [1] ss [2] green [3] green here [3] Shih[4]

# Contents

<b>Declaration of Authorship</b>	i
<b>Abstract</b>	iii
<b>Acknowledgements</b>	iv
<b>1 Introduction</b>	1
1.1 Imaging . . . . .	1
1.2 Two-Photon Imaging . . . . .	2
1.2.1 Two-Photon Imaging using entangled photon pairs . . . . .	3
1.2.2 Two-photon Imaging Using Thermal Sources . . . . .	3
1.2.3 Simulations . . . . .	4
<b>2 Theoretical Discussion</b>	5
2.1 Imaging . . . . .	5
2.2 Two-photon Imaging . . . . .	5
2.3 Light Source . . . . .	5
2.3.1 Biphoton . . . . .	5
2.3.2 Mode Function . . . . .	5
2.3.3 SPDC . . . . .	5
2.3.4 Phase matching conditions . . . . .	5
2.3.5 Gaussian approximations . . . . .	6
2.3.6 Fresnel Propagator . . . . .	6
2.4 Fourier Optics . . . . .	7
2.5 Spatial Correlations . . . . .	7
2.6 Measurement . . . . .	7
<b>3 Experimental Setup</b>	8
3.1 SPDC Setup . . . . .	8
3.1.1 Diode Laser . . . . .	8
3.1.2 Mirror . . . . .	8
3.1.3 Spatial Filter . . . . .	9
3.1.4 Waist Lens . . . . .	10
3.1.5 BBO(Beta Barium Borate) Crystal . . . . .	11
3.2 Spatial Correlations Measurement Setup . . . . .	11
3.2.1 Lens (Fourier Plane) . . . . .	11
3.2.2 Polariser . . . . .	12
3.2.3 Interferometer Filter . . . . .	12
3.2.4 Pin Hole(Arduino) . . . . .	12
3.2.5 Single Photon Counting Module(SPCM) . . . . .	12
3.2.6 Field-programmable gate array(FPGA) . . . . .	12
3.2.7 Computer(Data Analysis) . . . . .	12
3.3 Two-Photon Imaging Setup . . . . .	13

3.3.1	Mask	13
3.3.2	Folding Mirror	13
3.3.3	Bucket Detector	13
<b>4</b>	<b>Results</b>	<b>14</b>
4.1	Finding The Correlated Photons	14
4.2	Experimental Correlations	14
4.2.1	$w_p = ?$	14
4.3	Mask Alignment	14
4.4	Two-Photon Images	14
4.4.1	mask1	14
4.4.2	mask2	14
4.4.3	mask3	14
<b>5</b>	<b>Discussions and Conclusion</b>	<b>17</b>
<b>Bibliography</b>		<b>18</b>

# List of Figures

1.1	Optical imaging: a lens produces an image on an object at $f + d$ . This distance is defined by the Gaussian thin-lens equation $\frac{1}{f} + \frac{1}{f+d} = \frac{1}{f}$ . . . . .	2
1.2	Schematic of the first "two-photon imaging" experimental setup, used by Pittman[5] . . . . .	3
3.1	Image of the Diode Laser and it's control module, Taken from [6] . . . . .	8
3.2	Mirror and the cavity mount . . . . .	9
3.3	The spatial intensity profile before and after the spatial filtering process , Taken from [7] . . . . .	9
3.4	Basic elements of a Spatial Filter. In our experiment we use a Aspheric Lens of $f = 30mm$ (LA1805-A), a pinhole of $50\mu m$ and a collimating lens of $f = 60mm$ (LA1134-A). Taken from [7] . . . . .	10
3.5	This helps to form circular apertures of variable radius . . . . .	10
3.6	Lens' effect on a Gaussian beam . . . . .	10
3.7	Actual BBO crystal used in experiment . . . . .	11
3.8	Single Photon Counting Module . . . . .	12
3.9	Foldind Mirror, it is in the position for measuring the correlations . . . . .	13
4.1	We are moving the translational translational stage, to locate the spot where the correlated photon are, for this try me moved the y direction . . . . .	14
4.2	Localization of the mask with an square . . . . .	15
4.3	Moving the L Mask in order to put it in the most central spot . . . . .	15
4.4	Long exposure of the definitive localization of the mask, in this try we leave the detector in each place for 30 seconds, we also make the steps of the detector smaller, $0.1mm$ . . . . .	15
4.5	Localization of the mask with an square . . . . .	16

# List of Tables

# List of Abbreviations

**LAH** List Abbreviations Here  
**WSF** What (it) Stands For

# Physical Constants

Speed of Light  $c_0 = 2.997\,924\,58 \times 10^8 \text{ m s}^{-1}$  (exact)

# List of Symbols

$a$	distance	m
$P$	power	W ( $\text{J s}^{-1}$ )
$\omega$	angular frequency	rad

*For/Dedicated to/To my...*

## Chapter 1

# Introduction

Taking a photograph of an object, traditionally, we need to face a camera (detector) to the object. But with two-photon imaging we use a detector that is towards the light source, rather than towards the object. As the name suggests it, we also use the information about another photon that is strongly correlated. (IMAGE) Two-photon is reproduced at quantum level by a non-factorizable point-to-point image-forming correlation between two photons.

Two-photon imaging has been demonstrated using two types of light sources. Type-one two-photon imaging uses entangled photon pairs as the light source. In 1995 Pittman, realized a quantum two-photon geometric optical effect. They have successfully performed optical imaging by means of a quantum-mechanical entangled source[5].

Type-two of imaging uses chaotic light. The type-two image-forming correlation is caused by the superposition between paired two-photon amplitudes, or the symmetrized effective two-photon wave-function[8].

### 1.1 Imaging

Assuming we have an object that have its own light or its externally illuminated, imaging means collecting that light that is emitted from the object. Each point of the surface of the object will emit spherical waves to all possible directions, been this said, What is the probability to have a spherical wave collapsing into a point or small spot? Obviously, the chance is practically zero unless an imaging system is applied. The concept of optical imaging was well developed in classical optics and the Figure 1.1 schematically illustrates a standard imaging setup. In this setup an object is illuminated by a radiation source, an imaging lens is used to focus the scattered and reflected light from the object onto an image plane which is defined by the “Gaussian thin lens equation”[9]:

$$\frac{1}{s_0} + \frac{1}{s_i} = \frac{1}{f} \quad (1.1)$$

where  $s_0$  is the distance between the object and the imaging lens,  $s_i$  the distance between the imaging lens and the image plane, and  $f$  the focal length of the imaging lens. This equation defines a point-to-point relationship between the object plane and the image plane: any radiation starting from a point on the object will collapse at a certain point at the image plane.

This one-to-one correspondence in the image-forming relationship between the object and the image planes produces a perfect image. The observed image can be magnified or demagnified, for example, in the Figure 1.1 the original object is a tree, and it is demagnified at the image plane. This depends on which optical system are we using, what kind of lenses are involved and the distance between object and

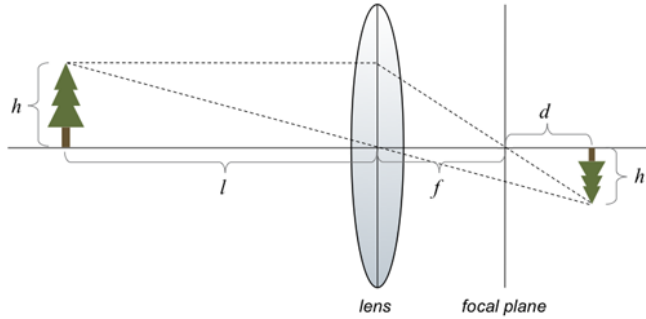


FIGURE 1.1: Optical imaging: a lens produces an image on an object at  $f + d$ . This distance is defined by the Gaussian thin-lens equation

$$\frac{1}{l} + \frac{1}{f+d} = \frac{1}{f}$$

them. The observed image is a reproduction of the illuminated object, mathematically corresponding to a convolution between the object distribution function  $|T(\vec{\rho}_o)|^2$  (aperture function) and a  $\delta$ -function, which is present for the perfect point-to-point correspondence[?]:

$$I(\vec{\rho}_i) = \int_{obj} d\vec{\rho}_o |T(\vec{\rho}_o)|^2 \delta(\vec{\rho}_o + \frac{\vec{\rho}_i}{m}) \quad (1.2)$$

where  $I(\vec{\rho}_i)$  is the intensity at the image plane,  $\vec{\rho}_o$  and  $\vec{\rho}_i$  are 2-D vectors of the transverse coordinates in the object and image planes, respectively, and  $m = s_i/s_o$  is the image magnification factor.

In reality, we are limited by the finite size of the optical system, we may never obtain a perfect image. we have to take into account the constructive-destructive interference present in this phenomena, because of the wave nature of light. The point-to-point correspondence turns into a point-to-"spot" relationship. For further informations about this "real life" situation check the ??.

## 1.2 Two-Photon Imaging

The optical imaging used the photons at the image plane to form the image, in other words it take measure one photon per spot at the image plane. For the type-one and type-two two-photon imaging, in certain aspects the behaviour is similar as that of the classical. They both exhibit a similar point-to-point imaging-forming function, except the two-photon image is only reproducible in the joint-detection between two independent photodetectors, and the point-to-point imaging-forming function is in the form of second-order correlation,

$$R_{12}(\vec{\rho}_i) = \int_{obj} d\vec{\rho}_o |T(\vec{\rho}_o)|^2 G^{(2)}(\vec{\rho}_o, \vec{\rho}_i) \quad (1.3)$$

where  $R_{12}(\vec{\rho}_i)$  is the joint-detection counting rate between photodetectors  $D_1$  and  $D_2$ .  $G^{(2)}(\vec{\rho}_o, \vec{\rho}_i)$  is a nontrivial point-to-point second-order correlation function, corresponding to the probability of observing a joint photo-detection event at the coordinates  $\vec{\rho}_o$  and  $\vec{\rho}_i$ . The physics behing  $G^{(2)}(\vec{\rho}_o, \vec{\rho}_i)$  is what changes between type-one and type-two two-photon imaging.

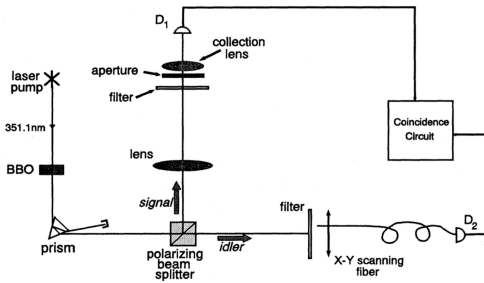


FIGURE 1.2: Schematic of the first "two-photon imaging" experimental setup, used by Pittman[5]

### 1.2.1 Two-Photon Imaging using entangled photon pairs

The first type-one two-photon imaging experiment was demonstrated by Pittman in 1995[5]. The schematic setup of the experiment is shown in the Figure 1.2. A continuous wave (CW) laser is used to pump a nonlinear crystal to produce pairs of entangled photons. This pairs of orthogonally polarized signal and idler photons are the product of the nonlinear optical process of spontaneous parametric down-conversion (SPDC). The pair emerges from the crystal collinearly, it is separated by a dispersion prism, and then the signal and idler are sent in different directions by a polarization beam slitting Glan-Thompson prism.

The experimental setup is shown in Fig. 1.A 2-mm-diam beam from the 351.1-nm line of an argon ion laser is used to pump a nonlinear beta barium borate (BBO) (P-BaBz04) crystal that is cut at a degenerate type-II phase-matching angle to produce pairs of orthogonally polarized signal (e-ray plane of the BBO) and idler (o-ray plane of the BBO) photons. The pairs emerge from the crystal nearly collinearly, with  $\theta = \pi/2$ . The pump is then separated from the slowly expanding down-conversion beam by a UV grade fused silica dispersion prism and the remaining signal and idler beams are sent in different directions by a polarization beam-splitting Thompson prism. The reflected signal beam passes through a convex lens with a 400-mm focal length and illuminates the (UMBC) aperture. Behind the aperture is the detector package  $D_1$ , which consists of a 25-mm focal length collection lens in whose focal spot is a 0.8-mm-diam dry ice cooled avalanche photodiode. The transmitted idler beam is met by detector package  $D_2$ , which consists of a 0.5-mm-diam multimode fiber whose output is mated with another dry ice cooled avalanche photodiode. Both detectors are preceded by 83-nm-bandwidth spectral filters centered at the degenerate wavelength 702.2 nm. The input tip of the fiber is scanned in the transverse plane by two orthogonal encoder drivers, and the output pulses of each detector, which are operating in the Geiger mode, are sent to a coincidence counting circuit with a 1.8-ns acceptance window.

An important fact of this experiment is the use of a lens(collection lens) in the signal beam that establishes an image plane with the definitive point-by-point correspondence object(mask) plane.

### 1.2.2 Two-photon Imaging Using Thermal Sources

In [10] they compared ghost Imaging using entanglement versus Classical correlated light. read and information in [11]. here i talk about coherence and intensity fluctuations [12]

### 1.2.3 Simulations

No[13]

## Chapter 2

# Theoretical Discussion

### 2.1 Imaging

### 2.2 Two-photon Imaging

### 2.3 Light Source

main source of information [8]

#### 2.3.1 Biphoton

$$|\Psi\rangle = \int dq_s dq_i d\Omega_s d\Omega_i x [\Phi(q_s, \Omega_s; q_i, \Omega_i) \hat{a}^\dagger(\Omega_s, q_s) \hat{a}^\dagger(\Omega_i, q_i) + \Phi(q_i, \Omega_i; q_s, \Omega_s) \hat{a}^\dagger(\Omega_s, q_s) \hat{a}^\dagger(\Omega_i, q_i)] |0\rangle \quad (2.1)$$

taken like it appears on [1]

Where  $\Phi(q_s, \Omega_s; q_i, \Omega_i)$  are the mode fuctions or Biphotons, a fuctions that contain all the information about the correlations.  $\hat{a}^\dagger(\Omega_n, q_n)$  the creation of a photon with tranverse momentum  $q_n$  and frequency  $\Omega_n$

#### 2.3.2 Mode Function

$$\Phi(q_s, \Omega_s; q_i, \Omega_i) \propto E_p(q_p, \Delta_0) B_p(\Omega_p) \mathcal{C}_{spatial}(q_s) \mathcal{C}_{spatial}(q_i) x \mathcal{F}_{frequency}(\Omega_s) \mathcal{F}_{frequency}(\Omega_i) \text{sinc}\left(\frac{\Delta_k \mathcal{L}}{2}\right) \quad (2.2)$$

where  $B_p(\omega_p^0 + \Omega_p)$  and  $E_p(q_p)$  are the frequency and transverse momentum distribution of the pump.  $\mathcal{C}_{spatial}(q_n)$  spatial filtering.  $\mathcal{F}_{frequency}(\Omega_n)$  frequency filter function.

#### 2.3.3 SPDC

[1]

#### 2.3.4 Phase matching conditions

$$\Delta_0 = q_s^y \cos \varphi_s + q_i^y \cos \varphi_i + k_s \sin \varphi_s - k_i \sin \varphi_i; \quad (2.3)$$

$$\Delta_k = k_p - k_s \cos \varphi_s - k_i \cos \varphi_i - q_s^y \sin \varphi_s + q_i^y \sin \varphi_i + (q_s^x + q_i^x) \tan \rho_0 \cos \alpha + \Delta_0 \tan \rho_0 \sin \alpha \quad (2.4)$$

where  $k_n = [(\omega_n^0 n_n / c)^2 - |q_n|^2]^{\frac{1}{2}}$  is the longitudinal wavevector inside the crystal.  $\varphi_s$  and  $\varphi_i$  are the propagation directions of the generated photons inside the crystal with respect to the pump direction  $z$  and  $\alpha$  is the azimuthal angle.

### 2.3.5 Gaussian approximations

[1]

Taking into account the Gaussian nature of the pump, that's  $E_p(q_p^x, q_p^y) \approx \exp\left[-\frac{w_p^2}{4}(q_p^{x^2} + q_p^{y^2})\right]$ . approximating the sinc function by a Gaussian function with the same width at  $\frac{1}{e^2}$  of its maximum, i.e.,  $\text{sinc}(x) \approx \exp(-\gamma x^2)$  with  $\gamma$  equal 0.193.

$$\mathcal{F}_{frequency}(\Omega_n) \approx \exp\left[-\frac{\Omega_n^2}{4\sigma_n^2}\right] \quad (2.5)$$

$$\tilde{\Phi}(q_s, q_i) = \int d\Omega_s d\Omega_i \mathcal{F}_s(\Omega_s) \mathcal{F}_i(\Omega_i) \Phi(q_s, \Omega_s; q_i, \Omega_i) \quad (2.6)$$

The Biphoton then takes a quadratic form:

$$\tilde{\Phi}(q_s, q_i) = N \exp\left[-\frac{1}{2}x^T A x + i b^T x\right] \quad (2.7)$$

where  $N$  is a normalization constant,  $x$  is a 4-dimensional vector defined as  $x = (q_s^x, q_s^y, q_i^x, q_i^y)$ ,  $A$  is a  $4 \times 4$  real-valued, symmetric, positive definite matrix and  $b$  is a 4-dimensional vector.  $A$  and  $b$  are defined from the phase-matching conditions of the SPDC process.  $x^T$  and  $b^T$  denote the transpose of  $x$  and  $b$ .  $A$  and  $b$  are functions that depend of all the relevant parameters in the experiment such as the length of the crystal  $L$ , pump waist  $w_p$ , creation angles inside the crystal  $\varphi_n$  and the width of the spectral filter  $\sigma_n$ .

A way to quantify the degree of spatial correlation we shall define 'correlation parameter':

$$K^\lambda = \frac{C_{si}^\lambda}{\sqrt{C_{ss}^\lambda C_{ii}^\lambda}} \quad (2.8)$$

calculated for each direction ( $\lambda = x, y$ ) from the covariance matrix  $C^\lambda$  with elements  $C_{kj}^\lambda = \langle q_k^\lambda q_j^\lambda \rangle - \langle q_k^\lambda \rangle \langle q_j^\lambda \rangle$ .

### 2.3.6 Fresnel Propagator

Fresnel Propagator:  $h(r, z) = (-\frac{i}{\lambda z}) e^{(i \frac{2\pi z}{\lambda})} \Psi(r, z)$  with  $\Psi(r, z) = e^{(i \frac{\pi}{\lambda z}) r^2}$ . Thin-lens transfer function  $L_f(r) = \Psi(r, -f)$

$$G = \int d^2r_1 \int d^2r_0 h(r_f - r_1, f) L_f(r_1) h(r_1 - r_0, f) \quad (2.9)$$

The propagation is done by determining the Green function[3] of the optical path by which the beam will travel. The biphoton function in terms of transverse momenta  $\Phi_1(q_s, q_i)$  after traveling through two arbitrary optical paths can be expressed in terms of the corresponding Green functions and the initial biphoton function  $\Phi(q_s, q_i)$  as:

$$\Phi_1(q_s, q_i) = G_s(q_s, r_1) G_i(q_i, r_2) \Phi(q_s, q_i) \quad (2.10)$$

$$\Phi_1(r_1, r_2) = \int d^2q_s d^2q_i \Phi_1(q_s, q_i) \quad (2.11)$$

Taking advantage of the 2-F system as a Fourier-Transform to reduce the amount of calculations. Solving 2.9 over  $r_0$  and  $r_1$  we have:

$$G(q, r_f) = Ce^{\frac{i\pi}{\lambda f}r_f^2}e^{\frac{i\lambda f}{4\pi}q^2}\delta(q - \frac{2\pi}{\lambda f}r_f) \quad (2.12)$$

where C is a complex constant that depends only on  $\lambda = 2\pi c$  and  $f$ . Then we can define the Green Functions for each path:

$$G_1(q_s, r_1) = G(q_s, r_1)xT(r_1) \quad (2.13)$$

$$G_2(q_i, r_2) = G(q_i, r_2) \quad (2.14)$$

Where  $T(r_1)$  is the transfer function of the object.

Gathering all the previous results we can obtain  $\Phi_1(r_1, r_2) = C^2 T(r_1)\Phi(\frac{2\pi}{\lambda f}r_1, \frac{2\pi}{\lambda f}r_2)$ , which describes the biphoton at the planes of the object and the scanning detector. It shows that the biphoton at the 2F plane in terms of  $r_1$  and  $r_2$  has the same form as the biphoton at the output face of the crystal with the relationship  $q = \frac{2\pi}{\lambda f}r$ . This allows to computationally simulate the biphoton at the 2-F plane by using Eq 2.7 without the need to computationally simulate its propagation through the 2-F system.

We are collecting all the light that interacts with the object by the means of a bucket detector, this from the mathematical point of view leave us with:  $\Phi_1(r_2) = C^2 \int d^2r_1 T(r_1)\Phi(\frac{2\pi}{\lambda f}r_1, \frac{2\pi}{\lambda f}r_2)$  The coincidence counts that will be measured by the Detectors will be proportional to the magnitude square of the resulting biphoton function  $\Phi_1(r_2)$ .

$$S(r_2) \propto |\int d^2r_1 T(r_1)\Phi(\frac{2\pi}{\lambda f}r_1, \frac{2\pi}{\lambda f}r_2)|^2 \quad (2.15)$$

For non-ideal forms of  $\Phi(q_s, q_i)$  we have the relation between  $\Phi(q) \rightarrow \Phi(r)$  for a 2F system, Hence:  $\Phi(r) = \frac{1}{\sqrt{\det(\Sigma)(2\pi)^4}} e^{-\frac{1}{2}r^T\Sigma^{-1}r} e^{ibr}$

$\Sigma =$

---

## 2.4 Fourier Optics

## 2.5 Spatial Correlations

[2] whenever i talk of spatial correlations and the especific case

## 2.6 Measurement

Paper about statistics of the measurement[14]

## Chapter 3

# Experimental Setup

### 3.1 SPDC Setup

#### 3.1.1 Diode Laser

The light source used in this experiment is a Diode Laser that delivers a continuous wave(CW) at  $\lambda = 406, 101\text{nm}$  and  $\Delta\lambda = 4\text{nm}$ . The laser model No. DL 405-200 delivers light at 200 mW with a beam diameter of 1.5 mm and a beam Divergence 1.2 mrad. IN HERE I MAY TALK ABOU THE M FACTOR, QUALITY PARAMETER OF GAUSIAN BEAMS  $M^2$  Power 200mW



FIGURE 3.1: Image of the Diode Laser and it's control module, Taken from [6]

#### 3.1.2 Mirror

further details to be asked,



FIGURE 3.2: Mirror and the cavity mount

### 3.1.3 Spatial Filter

A laser beam can be characterized by measuring its spatial intensity profile at points perpendicular to its direction of propagation. The spatial intensity profile is the variation of intensity as a function of distance from the center of the beam, in a plane perpendicular to its direction of propagation. In the Figure 3.3(top part) we see

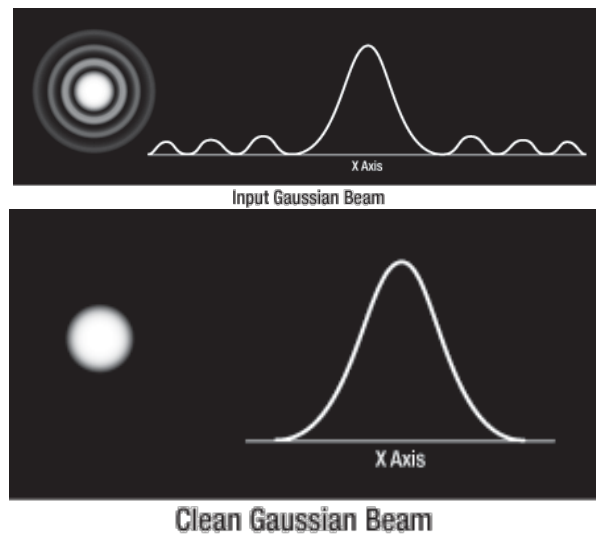


FIGURE 3.3: The spatial intensity profile before and after the spatial filtering process , Taken from [7]

the input gaussian beam and how its intensity fluctuates around the x axis. The output desired beam after going through the spatial filter is shown at the bottom of the Figure 3.3. The simplest arrangement to achieve this output spatial intensity profile is show in the Figure 3.4, where at the end we have a beam which intensity strength falls off transversely following a bell-shaped curve that's symmetrical around the central axis. Taking a closer look at the Figure 3.3(top part) we may recognise a

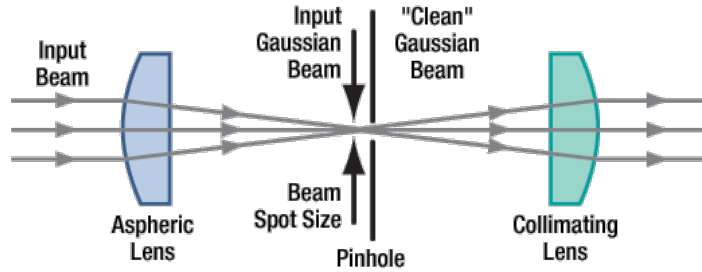


FIGURE 3.4: Basic elements of a Spatial Filter. In our experiment we use a Aspheric Lens of  $f = 30\text{mm}$ (LA1805-A), a pinhole of  $50\mu\text{m}$  and a collimating lens of  $f = 60\text{mm}$ (LA1134-A). Taken from [7]

diffraction pattern, but when we measure this spatial profile directly from the diode laser, we find out that it doesn't follow that behaviour, on the contrary it follows a more random spatial profile. This ramdom spatial profile is a result of the randomness in the quantum emissions and absorptions that are happening at the exited atoms at the diode laser[9].

In order to have this spatial intensity profile at the input of my lens arrangement, Figure 3.4, we put a circular aperture with the help of a pair of irises, Figure 3.5, before the  $f = 30.0\text{mm}$  lens and after the  $f = 60.0\text{mm}$  lens.



FIGURE 3.5: This helps to form circular apertures of variable radius

### 3.1.4 Waist Lens

A Gaussian beam hits a lens....To control the pump waist we can put a lens in the propagation direction with certain focal lenght  $f$ . This lens will define a zone around

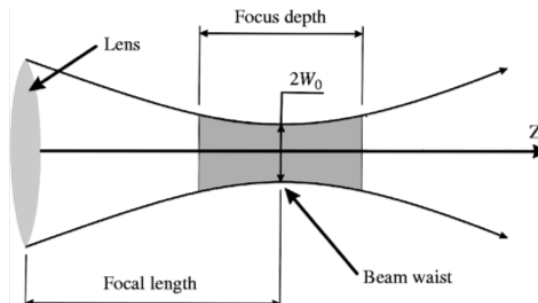


FIGURE 3.6: Lens' effect on a Gaussian beam

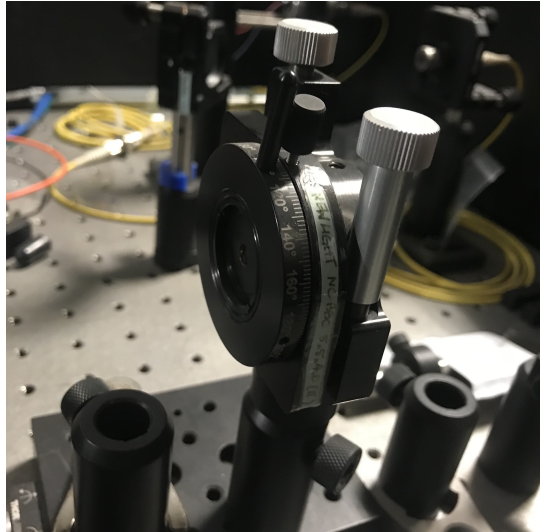


FIGURE 3.7: Actual BBO crystal used in experiment

the distance  $f$  called *Focus depth*[9] , where in the middle we find the narrowest point of the beam, Figure 3.6. The radius of this zone is:

$$W_0 = \frac{\lambda f}{\pi W_B} \quad (3.1)$$

Where  $W_B$  is the initial waist beam.

If we want to focus the beam at a fixed distance  $F$ , using this method to control the pump waist is not practical. Every different lens we would use will make this waist  $W_0$  at a different distances  $f$ . It is necessary to find a *Waist lens* that make us a waist  $W_0$  at a transverse plane located in a fixed position  $F$  from the *Waist Lens*. This special lens consists in an arrangement of two lenses, a positive and negative one respectively, separated a distance  $d_0$  from each other. SOURCE WHERE THEY EXPLAIN HOW TO USE A POSITIVE AND NEGATIVE ASK OMAR!!!

### 3.1.5 BBO(Beta Barium Borate) Crystal

the power of the pump is 60mW The nonlinear optical media used in this experiment is a BBO(Beta Barium Borate) crystal, this crystal is 5x5x4mm.

The crystal is mounted in such way that the input and output plane are fixed, Figure 3.7.

## 3.2 Spatial Correlations Measurement Setup

From this point we will talk about a pair of entangled photon pairs, that will come from the output plane of the BBO crystal, for historical reasons we will label this pairs as *signal* and *idler*.

### 3.2.1 Lens (Fourier Plane)

To define the  $2f$  system we use a lens(LA1708) of  $f = 200.0\text{mm}$  in front of each *signal* and *idler*. This lens is placed at a distance  $f$  from the output plane.

### 3.2.2 Polariser

In order to be able to filter certain polarisation direction we used a pair of Polarisers(WP25M-UB), which consist in a circular surface than only transmit the light that comes in a specific direction. other directions are reflected

### 3.2.3 Interferometer Filter

In this situation we are interested in the correlations in the space variables, hence we would like to filter al this time variables. To do this filtering we used a spectral filter(FB810-10) that only transmits the light that comes with  $\lambda = 810 \pm 2nm$ .

### 3.2.4 Pin Hole(Arduino)

MORE DETAILS, HOW MANY ARDUINOS, coupling lens refernece ETC ...

### 3.2.5 Single Photon Counting Module(SPCM)

To detect photons we a self-contained module that detects single photons of light over the  $400nm$  to  $1069nm$  wavelength range. The module used (SPCM-AQRH-13) uses a unique silicon avalanche photodiode (SLiK) with a detection efficiency of more than 65%[15]. Light is transmitted through a optic fiber from the pin hole detector to the SPCM. The result signal coming from the SPCM are pulses that represents one photon detections.



FIGURE 3.8: Single Photon Counting Module

### 3.2.6 Field-programmable gate array(FPGA)

Both *signal* and *idler* pulses from the respective SPCM goes to the same FPGA(ZestSC1). This Field-programmable gate array is programmed to count the photon coincidences, this means that the FPGA is fast enough to detect and separate pulses from photons that are time-separated.

### 3.2.7 Computer(Data Analysis)

labview is used to control the detection module, where is delivers a list of the detection, graph are made with any program language able to handle the data.

### 3.3 Two-Photon Imaging Setup

For the Two-photon imaging process we no longer have spatial information about the *signal* photon after it interacts with the mask

#### 3.3.1 Mask

This is an obstruction that is placed in the *signal* path with certain shape, it could be a mask with the shape of a letter or any other geometry. This is the object of which we want to construct an image.

#### 3.3.2 Folding Mirror

In order to change de path followed by the *signal* photon, we use a Folding mirror, Figure 3.9. This mirror can be in the *signal* path or not.



FIGURE 3.9: Foldind Mirror, it is in the position for measuring the correlations

#### 3.3.3 Bucket Detector

This detector consist in a coupling lens that collects all the light that goes through the mask, In contrast to the other detections made in this experiment, the Bucket detector loses track of any spatial information of the *signal* photon. Another big difference is that this Bucket detector uses a multimode optic fiber to take the light to the SPCM.

## Chapter 4

# Results

### 4.1 Finding The Correlated Photons

SPDC nocolinear type II

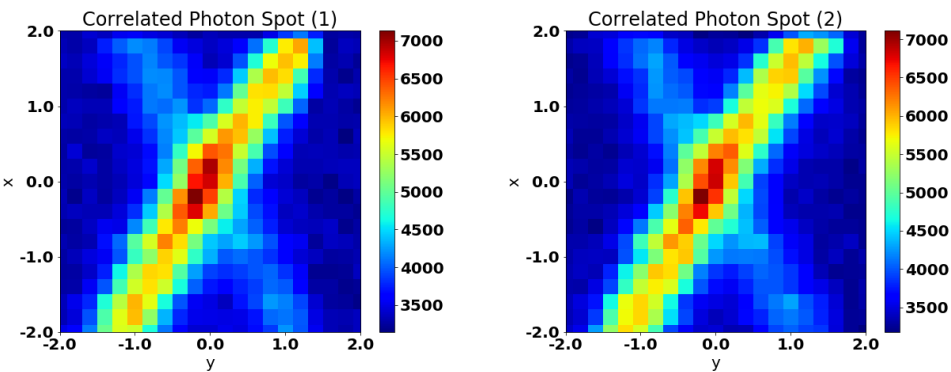


FIGURE 4.1: We are moving the translational translational stage, to locate the spot where the correlated photon are, for this try me moved the  $y$  direction

### 4.2 Experimental Correlations

Info taken before me

**4.2.1**  $w_p = ?$

### 4.3 Mask Alignment

We want that most of the correlated photon hits the mask  
changing to the mask with an L  
Long Exposure

### 4.4 Two-Photon Images

**4.4.1** mask1

**4.4.2** mask2

**4.4.3** mask3

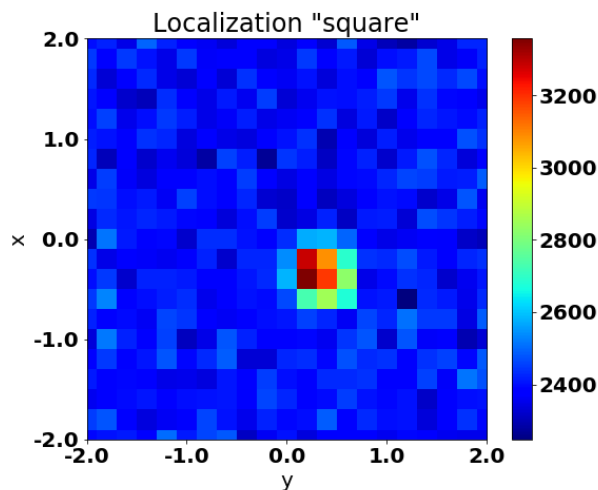


FIGURE 4.2: Localization of the mask with an square

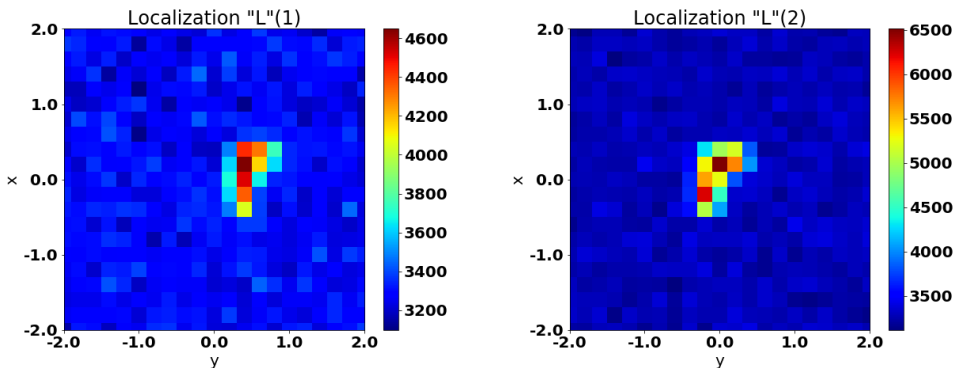


FIGURE 4.3: Moving the L Mask in order to put it in the most central spot

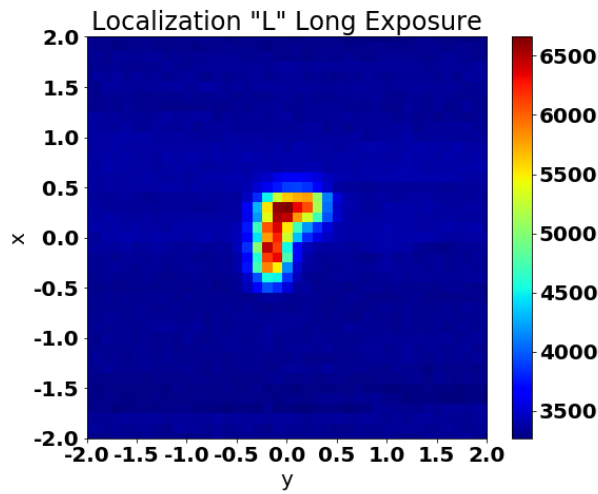


FIGURE 4.4: Long exposure of the definitive localization of the mask, in this try we leave the detector in each place for 30 seconds, we also make the steps of the detector smaller,  $0.1\text{mm}$

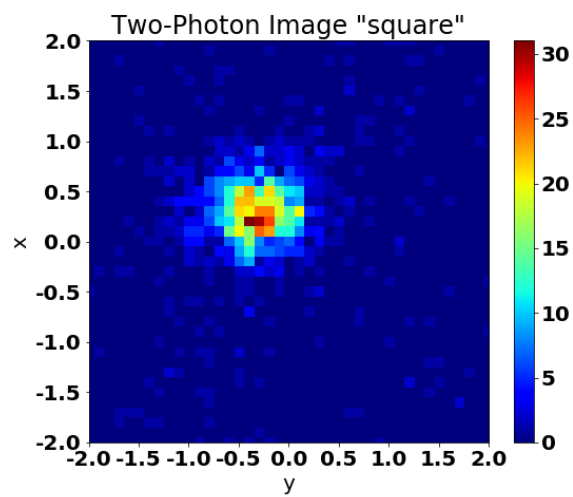


FIGURE 4.5: Localization of the mask with an square

## Chapter 5

# Discussions and Conclusion

# Bibliography

- [1] Clara I Osorio, Alejandra Valencia, and Juan P Torres. Spatiotemporal correlations in entangled photons generated by spontaneous parametric down conversion. *New Journal of Physics*, 10(11):113012, 2008.
- [2] Omar Calderón-Losada, Jefferson Flórez, Juan P. Villabona-Monsalve, and Alejandra Valencia. Measuring different types of transverse momentum correlations in the biphoton's fourier plane. *Opt. Lett.*, 41(6):1165–1168, Mar 2016.
- [3] Morton H. Rubin. Transverse correlation in optical spontaneous parametric down-conversion. *Phys. Rev. A*, 54:5349–5360, Dec 1996.
- [4] Y. Shih. *An Introduction to Quantum Optics: Photon and Biphoton Physics*. Series in Optics and Optoelectronics. Taylor & Francis, 2011.
- [5] T B. Pittman, Yanhua Shih, D V. Strekalov, and Alexander Sergienko. Optical imaging by means of two-photon quantum entanglement. *Physical review. A*, 52:R3429–R3432, 12 1995.
- [6] Crystal laser. <http://www.crystalaser.com>. Accessed: 2018-03-09.
- [7] Thorlabs, inc. <https://www.thorlabs.com/index.cfm>. Accessed: 2018-03-09.
- [8] Jeffrey H. Shapiro and Robert W. Boyd. The physics of ghost imaging. *Quantum Information Processing*, 11(4):949–993, Aug 2012.
- [9] E. Hecht. *Optics*. Pearson education. Addison-Wesley, 2016.
- [10] A. Gatti, E. Brambilla, M. Bache, and L. A. Lugiato. Ghost imaging with thermal light: Comparing entanglement and classicalcorrelation. *Phys. Rev. Lett.*, 93:093602, Aug 2004.
- [11] Alejandra Valencia, Giuliano Scarcelli, Milena D'Angelo, and Yanhua Shih. Two-photon imaging with thermal light. *Phys. Rev. Lett.*, 94:063601, Feb 2005.
- [12] W. Martienssen and E. Spiller. Coherence and fluctuations in light beams. *American Journal of Physics*, 32(12):919–926, 1964.
- [13] M. D'Angelo and Y. Shih. Can quantum imaging be classically simulated? *eprint arXiv:quant-ph/0302146*, February 2003.
- [14] J. H. Shapiro. The quantum theory of optical communications. *IEEE Journal of Selected Topics in Quantum Electronics*, 15(6):1547–1569, Nov 2009.
- [15] PerkinElmer. *Single Photon Counting Modules – SPCM*, 2010. Rev. 1.